COLLEGE OF ENGINEERING INDUSTRY PROGRAM

FACTORS AFFECTING THE FLUIDITY OF METALS

D. V. Ragone

This prepaper will be presented at the
Institute for Heat Transfer and Fluid Mechanics
at Los Angeles on June 25, 1955.

May, 1955

IP-116

SOME FACTORS AFFECTING FLUIDITY OF METALS

by

D. V. Ragone,* C. M. Adams,** and H. F. Taylor***

ABSTRACT

The fluidity of metals in the foundry sense (the distance that liquid metal can flow in a channel before being stopped by solidification) was studied both analytically and experimentally. Metal properties such as heat of fusion, heat capacity, viscosity, melting temperature and density were considered. The influence of test variables such as applied pressure head, channel diameter, and mold material properties was considered.

Analytically, equations were derived relating fluidity of pure metals to metal properties and test variables. Fluidity was found to vary directly with channel diameter, volumetric heat of fusion, applied pressure head, and superheat. Fluidity varied inversely with friction factor, temperature difference between metal and mold, and heat-absorbing ability of the mold. Change in viscosity was found to have but a small effect.

Some of these relationships were checked experimentally using a new fluidity test designed to conform with the conditions of the derivations.

---

*Submitted to the Department of Metallurgy, Massachusetts Institute of Technology, in partial fulfillment of the requirements for the degree of Doctor of Science; now, Assistant Professor of Metallurgical Engineering, University of Mi igan.

,*Assistant Professor and Professor of Metallurgy, respectively, at the Massachusetts Institute of Technology.

In order to discuss the subject of fluidity, there must first be a clarification of the ambiguous terms used in the field. The term "fluidity" has been used as a fundamental physical constant of materials (reciprocal of the viscosity). Foundrymen, however, have adopted the term and have changed the meaning somewhat. In the foundry sense, fluidity is an empirical measure of the distance a liquid metal will flow before it solidifies. The values of fluidity thus obtained are not fundamental physical constants of the metal, but are rather a function of many physical constants and of the variables of the test used. Fluidity values are generally given as distance flowed through a channel of particular cross section before solidification.

History of Fluidity Testing

T. D. West (37) in 1898 was the earliest investigator to report on the properties of molten metals as cast into sand molds. He poured metal into a horizontal wedge and considered the distance flowed as a measure of fluidity. Ledebure in 1904 (38), Sexton and Primrose (38) in 1911 and Moldenke in 1917 (39) modified the wedge test somewhat.

Ruff (26) ran metal in a long cylindrical channel and used the length flowed in the channel as his value of fluidity. This test was particularly sensitive to errors in leveling. Evans (6) has tried an inverted "U" type of test in which he uses several vertical sections of various cross-sectional areas fed from a common channel. The heights to which the metal rises in the various sections is a gauge of fluidity.

The familiar fluidity spiral was first tried by Saito and Hayaschi (40) in 1919. Their channel was wound into a spiral thereby simplifying handling and leveling problems. Many investigators have used and improved this spiral type of test, and it is now accepted in America as a standard for fluidity of iron and steel. (2, 6, 9, 11, 20, 27, 28, 32, 34, and 41) Eastwood and Kempf (5) have used a spiral casting of flat cross section for studying aluminum and its alloys. Because the length of such a spiral is not well defined, they use the volume of metal in the channel as a measure of fluidity.

THE VARIABLES

The variables that affect the fluidity data may be divided into three broad classifications; the inherent properties of the metal, the extrinsic properties of the metal, and the variables of the test equipment.

Properties of the Liquid

The intrinsic properties of the liquid which have significant effects on its fluidity are heat content (enthalpy), composition, surface tension, and viscosity. The literature is consistent with respect to the effect of heat content (2, 10, 18, 19, 20-25, 32). Fluidity varies directly with

heat content measured in terms of superheat (temperature increment above the liquidus). The effect of composition on fluidity has been investigated by pouring metal at a constant temperature interval above the liquidus across binary and ternary systems (20-25, 10). The results of these tests indicate that the fluidity is inversely proportional to the solidification interval (liquidus temperature--solidus temperature). The explanation advanced for this behavior hinges on the manner of solidification of the alloy. In the case of a pure metal or eutectic, the metal solidifies with smooth regular interfaces inward from the mold wall. Alloys with a solidification range solidify by forming dendrites which impair flow considerably.

It seems logical that variations in surface energy should affect the fluidity of a metal. In pouring the test, a new surface is being created which requires a source of energy. This source must be the moving stream of metal. This energy sink, however, proves to be a small one.

The question of whether or not the fluidity tests are viscosity-sensitive has been the subject of much discussion. Desch (4) and Briggs (34) hold that viscosity has no effect, while some other authors hold the opposite view (9, 35, 36). The opinions of the above authors are based on experimental data. This investigation treats the subject from an analytical point of view.

Extrinsic Properties of the Liquid

Dissolved gas, surface oxide films, and insoluble impurities can affect fluidity. Dissolved gases can either change physical properties of the metal such as viscosity, or provide shear mechanical interference as the gas comes out of solution upon solidification. The properties of oxide films that must be considered are the strength and specific gravity of the film and whether the film is solid or liquid at the casting temperature. A solid oxide film (such as that on aluminum) might form a continuous envelope around the stream and restrict its flow, or the film might be torn apart and mixed with the moving stream which would increase the effective viscosity. It has been found that solid films increase, and liquid films decrease the fluidity (9).

Variables of the Test Equipment

The casting system for a fluidity spiral consists of (Fig. 1) (1) a pouring basin and a downgate, (2) a "cushion" to dissipate kinetic energy of the falling stream, and (3) a spiral channel. Among the important test variables are the channel shape, design of the cushion, molding materials, and pouring rate. Greene (8) has shown that fluidity varies inversely as the perimeter to cross-sectional area ratio of the channel. Andrew et. al. (1), investigating the effect of cushion design, have demonstrated that under similar casting conditions different cushion designs gave fluidity values that varied by as much as a factor of two. The thermal diffusivity of the mold material, mold temperature, and pouring speed all influence fluidity (3, 9, 11, 20, 28, 32, 41). Spiral length varies directly with pressure head applied (9), hence it is not unreasonable to assume that the length would vary with the

rate of application of pressure head. The difficulties involved in controlling the above mentioned variables make it almost impossible to compare the data of the various authors.

Quantitative Contributions

Ruff (26) evaluated friction factors in steel flowing in a straight, cylindrical channel and found them to correspond closely to those predicted by the Reynolds number correlation. Portevin and Bastein (20-25) derived an equation which fits their data involving emperical constants which are a function of the equipment used. Taylor and Rightmire (33) have derived the relationship between fluidity and temperature of the metal and some equations for evaluating friction forces. These show good correlation. However, their data is taken from many investigators and is difficult to evaluate.

The purpose of the present investigation is to relate quantitatively fluidity to fundamental properties of metals, molding materials and test equipment design. Specifically, the plan is to derive analytically equations relating the fluidity of pure metals to the above mentioned properties and to conduct controlled experiments to check these relationships.

ANALYSIS OF SOLIDIFICATION IN A CYLINDRICAL MOLD

This section deals with heat transfer from a cylindrical mold, namely, the fluidity spiral channel. The analysis deals with a pure metal at its melting point, with the result that any heat withdrawn from the mold results in the solidification of some metal. A relationship is derived for the radius of the liquid stream at a point in the channel as a function of time of contact between the mold and the metal. Two different modes of heat transfer are considered.

In both of the following cases, the following assumptions are made:

1. The liquid metal is at its melting point.
2. There is no supercooling.
3. Metal solidifies on the inside of tube with smooth interface.
4. Metal that has frozen out provides no barrier to heat transfer.

Case I, (h-type)

In this case the main resistance to heat flow is at the inner surface of the tube, that is, at the mold-metal interface. This analysis applies to situations where the channel diameter is small (ratio of surface to volume is high) and when the mold material may be considered a chill. q, the amount of heat transferred through this surface per unit time is:

$$q = hA(T_s - T_r) \qquad \text{(A-1)}$$

Consider the element dL in Fig. 2. In time $d\theta$, the element dr freezes out.

$$dQ_1 = 2\pi r \rho H_f \, dr \, dL \qquad (A\text{-}2)$$

and

$$dQ_2 = - h(T_s - T_r) \, 2\pi a \, d\theta \, dL \qquad (A\text{-}3)$$

where:

dQ_1, dQ_2 = Differential quantities of heat as indicated on Fig. 2
r,a,L = Dimensions as indicated on Fig. 2
h = Heat transfer coefficient as defined by Eq. (A-1)
ρ = Density of metal
H_f = Heat of fusion of metal (cal/gram)
T_s = Equilibrium solidification temperature of metal
T_r = Room temperature, that is, the initial temperature of the mold or tube.

since $dQ_1 = dQ_2$,

$$rdr = - ah \left(\frac{T_s - T_r}{\rho H_f} \right) d\theta \qquad (A\text{-}4)$$

Integrating

$$r^2 = a^2 - 2ah \left(\frac{T_s - T_r}{\rho H_f} \right) \theta \qquad (A\text{-}5)$$

The time for final solidification θ_f is (r = 0):

$$\theta_f = \frac{a}{2h} \left(\frac{\rho H_f}{T_s - T_r} \right) \qquad (A\text{-}6)$$

For purposes of notation let

$$\beta = \frac{2h(T_s - T_r)}{\rho H_f} \qquad (A\text{-}7)$$

Then

$$r^2 = a^2 - a\beta\theta \qquad \text{(A-8)}$$

$$\theta_f = \frac{a}{\beta} \qquad \text{(A-9)}$$

Case II (θ-type)

In this case the main resistance to heat flow arises in the mold. This analysis applies to situations where the mold material is an insulator. Sand molds fall into this category. This case has been treated by Adams (43) who gives as a very good approximation of the heat transferred into the mold:

$$q = A(T_s - T_r) \left(\frac{K' \rho' C_p'}{\pi}\right)^{1/2} \theta^{-1/2} \qquad \text{(A-10)}$$

where:

K' = Thermal conductivity of the mold
ρ' = Density of the mold material
C_p' = Heat capacity of the mold material
θ = Time after contact of the metal and mold.

For purposes of notation let

$$\gamma = 4 \left(\frac{K' \rho' C_p'}{\pi}\right)^{1/2} \frac{(T_s - T_r)}{\rho H_f} \qquad \text{(A-11)}$$

Again referring to Fig. 2

$$dQ_1 = 2\pi r \rho H_f \, dr \, dL \qquad \text{(A-2)}$$

$$dQ_2 = -2\pi a (T_s - T_r) \left(\frac{K' \rho' C_p'}{\pi}\right)^{1/2} \theta^{-1/2} \, d\theta \, dL \qquad \text{(A-12)}$$

Following the same pattern as in the previous case:

$$r^2 = a^2 - a\gamma\theta^{1/2} \tag{A-13}$$

$$\theta_f = \frac{a^2}{\gamma^2} \tag{A-14}$$

ANALYSIS OF FLOW IN A TUBULAR MOLD WITH SOLIDIFICATION

The system being considered in this section is illustrated in Fig. 3. The assumptions made in this analysis are:

1. The fluid is continuous.
2. The pressure P_e is constant.
3. The effects of acceleration may be neglected.

Taylor and Rightmire (33) have performed an analysis of this last assumption and have shown it to be quite justifiable (accurate to within 2%).

With the acceleration terms neglected, the equations of motion reduce to a total energy balance for the steady state (B-1)

$$Z_1 + \frac{V_1}{2g} + \frac{P_1}{\rho} = Z_2 + \frac{V_e^2}{2g} + \frac{P_e}{\rho} + \int_o^{L_e} \frac{fV^2}{2rg}\, dL \tag{B-1}$$

where:

g	=	Acceleration of gravity
$Z_e - Z_1$	=	Difference in height between E and 1
$P_e - P_1$	=	Difference in pressure between E and 1
ρ	=	Density of metal
V_e	=	Velocity at the end of the stream
V	=	Local average velocity across any cross section of the tube
r	=	Local radius of tube
f	=	Friction factor.

For purposes of notation:

$$2g\left[(Z_1 - Z_e) + \frac{P_1 - P_e}{\rho}\right] = H \qquad \text{(B-2)}$$

Since the area of the reservoir is large compared to the cross section of the tube, $V_1 = 0$. Eq. (B-1) reduces to:

$$V_e^2 + \int_o^{L_e} \frac{fV^2}{2r}\, dL = H \qquad \text{(B-3)}$$

With continuity, $AV = A_e V_e$

$$\pi r^2 V = \pi a^2 V_e; \qquad V = V_e \frac{a^2}{r^2} \qquad \text{(B-4)}$$

where a = radius of container. At the end of the liquid column (point e) the diameter of the liquid stream is the diameter of the container. Substituting (B-4) into (B-3):

$$V_e^2 \left(1 + \int_o^{L_e} \frac{fa^4}{2r^5}\, dL\right) = H \qquad \text{(B-5)}$$

With the metal at its melting point flowing into a tube, after a time Θ, the situation illustrated in Fig. 4 exists. As time Θ increases, L_e increases, r_o decreases until finally at $\Theta = \Theta_f$ (Eq. A-6, A-15), $r_o = 0$ and flow ceases. Thus the mechanism by which the moving stream is stopped is a "choking off" phenomenon occurring near the beginning of the stream.

In order to solve Eq. (B-5); assume:

$$r = r_o + \frac{a - r_o}{L_e} L \qquad \text{(B-6)}$$

Assume too that the friction factor, f, is constant. Both these assumptions are justified in Appendix C. The friction term of (B-5) can now be simply evaluated.

$$\int_0^{L_e} \frac{fa^4}{2r^5}\,dL = \frac{f}{8r_o^4}\left(\frac{a^4 - r_o^4}{a - r_o}\right) \qquad \text{(B-7)}$$

Eq. (B-5) then becomes

$$V_e^2\left(1 + \frac{f}{8r_o^4}\left[\frac{a^4 - r_o^4}{a - r_o}\right] L_e\right) = H \qquad \text{(B-8)}$$

or

$$\left(\frac{dL_e}{d\theta}\right)^2\left(1 + \frac{f}{8r_o^4}\left[\frac{a^4 - r_o^4}{a - r_o}\right] L_e\right) = H \qquad \text{(B-9)}$$

since $$H = V_o^2;$$

$$\left(\frac{dL_e}{d\theta}\right)^2\left(1 + \frac{f}{8r_o^4}\left[\frac{a^4 - r_o^4}{a - r_o}\right] L_e\right) = V_o^2 \qquad \text{(B-10)}$$

Eqs. (A-5) and (A-16) give $r_o = f(\theta)$. Eq. (B-10) becomes an equation in L_e and θ which can be solved in various fashions.

SOLUTION FOR L_e AS A FUNCTION OF θ

Case I (Friction factor f = 0)

The integration of Eq. (B-10) yields

$$L_e = V_o\theta \qquad \text{(C-1)}$$

and $$L_f = V_o \theta_f$$

where L_f is the final length. For h-type heat transfer

$$L_f = V_o \frac{a}{\beta} = V_o \frac{a}{2h} \frac{\rho H_f}{T_s - T_r} \tag{C-2}$$

For θ-type

$$L_f = V_o \frac{a}{\gamma^2} = V_o \frac{a^2}{4} \frac{\pi}{K' \rho' C_p'} \left[\frac{\rho H_f}{T_s - T_r} \right]^2 \tag{C-3}$$

Case II (Constant friction factor)

The equation (B-10) can be solved by either a numerical method (modified Euler technique) (45) or by application of Simpson's rule (46). To use the modified Euler technique, increments were taken in the independent variable, θ. Through the use of equation (A-5), the factor $f(a^4-r_o^4)/8r_o^4(a-r_o)$ was evaluated as a function of θ. Successive approximations to L_e as a function of θ were made as outlined in Appendix A. The solution converges very rapidly and is quite stable after the fifth approximation. Fig. 5 lists the solutions to the equation for several values of friction factor.

Application of Simpson's rule provides another solution to equation (B-10). (See Appendix B) In order to apply this rule, it is first necessary to assume a form of $L_e = f(\theta)$. The numerical integrations have shown that a reasonable approximation is:

$$V_e = \left(1 + \frac{\theta}{\theta_f}\right) V_o \tag{C-10}$$

since $$L_e = \int_o^\theta V_e d\theta \,, \tag{C-11}$$

$$L_e = \frac{1}{2} \frac{V_o}{\theta_f} \left[\theta_f^2 - (\theta_f - \theta)^2 \right] \tag{C-12}$$

Eq. (B-10) becomes

$$\left(\frac{dL_e}{d\theta}\right)^2 \left[1 + \frac{f}{8r_o}\left(\frac{a^4 - r_o^4}{a - r_o}\right)\left(\frac{1}{2}\frac{V_o}{\theta_f}\right)\left(\theta_f^2 - (\theta_f - \theta)^2\right)\right] = V_o^2 \qquad (C\text{-}13)$$

The solution to (C-13) is simplified if the independent variable is changed from θ to r_o. Considering the h-type of heat transfer, this substitution yields:

$$\frac{dL_e}{dr_o} = -\frac{2\,V_o\,r_o}{a\beta}\left[1 + \frac{f}{16}\left(\frac{a^4 - r_o^4}{a - r_o}\right)\left(\frac{V_o}{a^2\beta\, r_o^4}\right)\right]^{-1/2} \qquad (C\text{-}14)$$

$$L_f = -\frac{2V_o}{a\beta}\int_a^o \left[1 + \frac{f}{16}\left(\frac{a^4 - r_o^4}{a - r_o}\right)\left(\frac{V_o}{a^2\beta\, r_o^4}\right)\right] r_o dr \qquad (C\text{-}15)$$

Applying Simpson's Rule (4 parts)

$$L_f = \frac{V_o a}{\beta} F\left(\frac{V_o f}{\beta}\right) \qquad (C\text{-}16)$$

where

$$F\left(\frac{V_o f}{\beta}\right) \equiv \frac{1}{6}\left[1 + \left(1 + 21.3\,\frac{V_o f}{\beta}\right)^{-1/2} + \left(1 + 1.76\,\frac{V_o f}{\beta}\right)^{-1/2} + \left(1 + .370\,\frac{V_o f}{\beta}\right)^{-1/2}\right]$$

Fig. 6 is a plot of $F(V_o f/\beta)$ vs. $(V_o f/\beta)$, and Fig. 7 gives L_f as a function of V_o/β for various values of f. The table in Appendix B shows that these values calculated using Simpson's Rule are quite close to those determined by the modified Euler method. This provides justification for approximation (C-10).

A similar analysis for the case of θ-type heat transfer yields

$$L_f = \frac{V_o a^2}{\gamma^2} G\left(\frac{f\,V_o\,a}{\gamma^2}\right) = \frac{V_o a^2}{\gamma^2} G(D)$$

Fig. 8 is a plot of G(D) vs. D.

THE EFFECT OF SUPERHEAT ON FLUIDITY OF A PURE METAL

Commercially, metals are never poured at their melting points. It becomes necessary thus to consider the effect of superheat on fluidity.

In order to treat analytically superheated metals, it is convenient to deal with the problem in two steps: first, the stage in which the metal in the mold cools off to the melting point (no solidification) and second, the process of solidification. Let the length attained by the metal in stage one be L_1 and the distance flowed after solidification has begun be L_2. To simplify the analysis, assume that the two stages are independent so that

$$L_f = L_1 + L_2 \tag{D-1}$$

To solve for L_1, it is necessary to consider the equation of flow once again. (B-3) In stage one with no solidification, $V = V_e$ and $r = a$. With f constant

$$V_e = V_o \left(1 + \frac{f}{2a} L_e\right)^{-1/2} \tag{D-2}$$

$$\left(1 + \frac{f}{2a} L_e\right)^{1/2} dL_e = V_o \, d\theta \tag{D-3}$$

Integrating

$$\frac{4}{3} \frac{a}{f} \left[\left(1 + \frac{f}{2a} L_e\right)^{3/2} - 1\right] = V_o \, \theta \tag{D-4}$$

Assuming that the thermal situation is governed by the h-type of heat transfer, a heat balance is performed for a differential element of the tube dL.

$$d\theta = \left(\frac{a}{2}\right)\left(\frac{\rho C_p}{h}\right) \frac{dT}{T - T_r} \tag{D-5}$$

Case I (no friction)

With no friction (f = 0) Eq. (D-2) reduces to:

$$d\theta = \frac{dL}{V_o}$$

Combining with Eq. (D-7) and integrating:

$$\int_0^{L_1} dL = \int_{T_o}^{T_s} \frac{1}{2} \frac{a\ V\ \rho C_p}{h} \frac{dT}{T - T_r}$$

where T_o = pouring temperature.

Assuming ρ, C_p, and h are not functions of temperature:

$$L_1 = \frac{1}{2} \frac{a\ V_o\ \rho\ C_p}{h} \ln \left(\frac{T_o - T_r}{T_s - T_r} \right) \tag{D-6}$$

Combining Eqs. (D-6), (D-1), and (C-4):

$$L_f = \frac{1}{2} \frac{a\ V_o}{h} \left[\rho\ C_p \ln \frac{T_o - T_r}{T_s - T_r} + \rho H_f \frac{1}{T_s - T_r} \right] \tag{D-7}$$

Case II (with friction factor constant)

Combining Eqs. (D-3) and (D-5):

$$\left(1 + \frac{f}{2a} L_e \right)^{1/2} dL_e = \frac{1}{2} \frac{V_o\ a\ \rho C_p}{h} \frac{dT}{T - T_r}$$

Integrating

$$L_1 = \frac{2a}{f} \left[\left\{ \frac{3}{8} \frac{f\ V_o\ \rho C}{h} \ln \left(\frac{T_o - T_r}{T_s - T_r} \right) + 1 \right\}^{2/3} - 1 \right] \tag{D-8}$$

For purposes of notation:

$$\propto \equiv \frac{3}{8} \frac{f\ V_o\ \rho\ C_p}{h}$$

$$T' \equiv \frac{T_o - T_r}{T_s - T_r} \tag{D-9}$$

To find L_2, the velocity at the point L_1 (V_1) must be known. From Eq. (D-2):

$$V_1 = V_o \left(1 + \frac{f}{2a} L_1\right)^{-1/2}$$

This velocity may be used to calculate L_2 from Eq. (C-19). Combining Eq. (D-1), (D-10) and (C-19):

$$L_f = \frac{2a}{f} \left[(\alpha \ln T' + 1)^{2/3} - 1\right] + \frac{V_1 a}{\beta} F\left(\frac{V_1 f}{\beta}\right) \qquad \text{(D-10)}$$

Eq. (D-12) is too involved to show directly the effects of the variables of interest. For this reason Eq. (D-10) was evaluated for various values of T', f, and a. The properties of the metal and of the test assumed were:

$$\frac{\rho H_f}{T_s - T_r} = .400 \text{ cal/cm}^3$$

$$\rho C_p = .800 \text{ cal/cm}^3 \text{ °C}$$

$$h = .25 \text{ cal/cm}^2 \text{ °C sec}$$

$$V_o = 250 \text{ cm/sec}$$

These are average values selected for the properties of most of the common metals and from experimental determinations. Fig. 9 shows L_f as a function of T' for various values of a.

Fig. 10 shows L_2/L_f as a function of T'.

EXPERIMENTAL PROCEDURE

In order to evaluate the relationships derived in the previous sections, it was necessary to devise a new fluidity test. The equations were derived assuming a constant and instantaneously-applied pressure head ($P_e - P_2$). It is obvious that this condition could not be met by the present fluidity test

in which the application of pressure head is not only noninstantaneous but also varies from test to test if the pouring rate varies. A simple test that fulfills the requirements was devised (Fig. 11). The normal spiral channel was replaced by a Pyrex tube (Vycor or silica tubes may be used). The pressure head was provided not by a head of metal, but rather by an adjustable partial vacuum applied to one end of the tube. The other end was bent to allow metal to be introduced into the tube while keeping the main portion of the tube level. Instantaneous application of the vacuum (pressure head) was achieved by sealing the entrance of the tube with a thin wafer of wax. Before the test was run, the vacuum was applied. When the entrance to the tube was dipped into the metal, the wax melted and the pressure instantaneously applied. To keep the pressure constant in the tube during the test, a vacuum resevoir was provided close to the other end of the channel. The vacuum was provided by an aspirator, controlled by a Cartesian Manostat, and measured with a mercury manometer.

The effective head of metal (ΔP_m) was determined as follows:

$$\Delta P_m = \Delta PH_g \frac{\rho H_g}{\rho_m} - \Delta Z \qquad \text{(E-1)}$$

$$V_o^2 = H = 2g \Delta P_m \qquad \text{(E-2)}$$

where:

ΔPH_g = Difference in pressure between inside of tube and atmosphere, measured in inches of mercury

ΔP_m = Effective head of metal measured in inches

ρH_g = Density of mercury

ρ_m = Density of metal

ΔZ = Difference in height between metal level in crucible and the level of the channel, measured in inches

The pure metals investigated were tin, lead and zinc. The criterion of purity was whether or not the metal solidified with a smooth interface. This was determined by numerous pour-out tests with cold graphite crucibles as the molds. The purity of the tin was at least 99.90 per cent, of the lead 99.95 per cent and of the zinc 99.9 per cent. The Pyrex tubes used as molds were sized on the inside diameter to within 0.002 inch of their stated size. Pressure was controlled to within $\pm$0.1 cm of mercury and the temperature measured to within 2°C. To determine L_e as a function of time, and the total freezing time, motion pictures were taken of the course of the fluidity test. A camera speed of 64 frames per second was used. The values of length were read in each frame on a standard Microfilm reader.

EXPERIMENTAL RESULTS

Using tin, fluidity was measured as a function of temperature for four different tube diameters. These data are presented in Fig. C-1 in Appendix C. Motion pictures were taken of most of the tests and from them values of final freezing time were obtained. These are plotted as a function of temperature for the various tube diameters in Fig. C-2. Extrapolation of the values of θ_f to the melting temperature gives the value of freezing time for metal poured at the melting point ($\theta_{f(m.p.)}$. From the values of $\theta_{f(m.p.)}$, assuming h-type of heat transfer, values of h were calculated from Eq. (A-7). From Eq. (C-16) the fluidity at the melting point was calculated as a function of tube diameters. The results of the calculations are given below and are plotted as fluidity at the melting point vs. tube diameter in Fig. 12.

TABLE I

FLUIDITY OF TIN AT MELTING POINT AS A FUNCTION OF TUBE SIZE

P_m = 10 inches; V_o = 222 cm/sec

P_{Hg} = 7.25 inches; f = 0.023

a (cm)	$\theta_{f(m.p.)}$ (sec)	h (calculated) (cal/sec-cm^2)	L_f (calculated) (cm)	L_f (observed) (cm)
0.281	.453	.160	46.2	49.5
0.230	.391	.152	38.1	41.4
0.187	.308	.157	30.7	29.7
0.161	.247	.168	26.2	25.0
		avg. 0.159		

Fig. 13 shows for one test (conditions listed on figure) the length as a function of time during the course of the test. There is good agreement between observed and calculated curves. (The calculated curve was the result of a numerical integration as in Appendix A.)

Table II presents calculated and observed values for the fluidity of zinc and lead at their melting points.

TABLE II

Metal	a	V_o	h	L_f (calculated) (cm)	L_f(observed) (cm)
Pb	.234	222	.098	31.7	28.9
Zn	.230	222	.0802	53.6	56.0
Zn	.155	289	.0802	44.0	42.5
Zn	.203	289	.0802	57.5	57.3
Zn	.240	289	.0802	68.5	71.2

In order to evaluate Eq. (D-10) which gives fluidity as a function of temperature for h-type heat transfer, metal tubes were used for the test. Metallic tubes provide a greater chill than glass tubes (they have a better thermal conductivity) and thus make contact resistance a larger portion of the total resistance to heat transfer. These metal tubes were bent and sealed with wax as the glass tubes were. Final length was determined by cutting the tubes open. The value of h was calculated from the fluidity at the melting point (extrapolation) by Eq. (C-16). This value was used in Eq. (D-10) to determine fluidity as a function of temperature. The resulting calculated curve and the data are shown in Fig. 14.

CONCLUSIONS

From Analytical Approach

For pure metals, in cases in which the main resistance to heat flow is at the mold-metal interface (chill mold or molds of small diameter):

1. Fluidity is a linear function of tube diameter.

2. Fluidity at the melting point is a function of the dimensionless term $V_o(\rho H_f)/h(T_s-T_r)$ and of its product with the friction factor $V_o f(\rho H_f)/h(T_s-T_r)$.

3. The effect of superheat on fluidity is related to the dimensionless product $fV_o\rho C_p/h$ and to the natural logarithm of the relative temperature $(T_o-T_r)/(T_s-T_r)$.

4. The effect of changes in viscosity is small. Since the flow is turbulent,

$$f = 0.185 \left(\frac{DV_o}{\mu}\right)^{-0.20}$$

$$\frac{\Delta f}{f} = 0.20 \left|\frac{\Delta \mu}{\mu}\right|$$

Values of f normally fall between 0.02 and 0.03. Using Fig. 9 and the above equation (for f = 0.025), a change of 50 per cent in viscosity ($\Delta\mu/\mu = 0.50$) amounts to an average of 2.6 per cent change in fluidity.

5. The portion of the total fluidity contributed by the metal after it has reached the melting point is considerable.

For pure metals at their melting point in cases where the main resistance to heat flow is in the mold itself (insulating molds or molds with large channels):

1. Fluidity is a function of the dimensionless term $\frac{V_o a}{K'\rho'C_p'}\left(\frac{\rho H_f}{T_s - T_r}\right)^2$ and of its product with the friction factor $\frac{V_o f a}{K'\rho'C_p'}\left(\frac{\rho H_f}{T_s - T_r}\right)^2$.

2. For different metals, the fluidity in an insulator such as a sand mold should vary roughly as the square of the volumetric heat of fusion divided by the difference between the melting point and the mold temperature $\left(\frac{\rho H_f}{T_s - T_r}\right)^2$.

3. Changes in viscosity have a small effect on fluidity.

4. Fluidity varies roughly as the square of channel diameter.

From Experimental Approach

For pure metals:

1. Assuming that the main resistance to heat flow is contact resistance, fluidity at the melting point can be successfully predicted in lower-melting metals in glass tube molds.

2. Fluidity is not zero at the melting point. This was determined both from extrapolation to and direct measurement at the melting point. Even when the metal is highly superheated, a substantial portion of the total fluidity is contributed by the metal after it has reached its melting point.

BIBLIOGRAPHY

1. Andrews, Percival and Bottomley, Iron and Steel Institute, Special Report No. 15 (1936).

2. Clark, K. L., Proceedings of the Institute of British Foundrymen, 39, A52, Paper 847 (1945/6).

3. Courty, Revue de Metallurgie, 28, 169 (1931).

4. Desch, S. H., Foundry Trade Journal, 56, 505, June 17, 1937.

5. Eastwood and Kempf, Transactions of the American Foundrymen's Association, 47, 571-582 (1939).

6. Evans, Journal of Research and Development of the British Cast Iron Research Association, Research Report 319, October, 1951.

7. Greenaway, H. T., Journal of the Institute of Metals, Paper 1115, 74, 133, (1947/8).

8. Greene, R. H., Iron and Steel Institute, Special Report No. 15 (1936).

9. Kondic, V., Foundry Trade Journal, 88, 691, June 27, 1950.

10. Kondic, V. and Kozowski, H. J., Journal of the Institute of Metals, Paper 1174, 75, 665 (1948/9).

11. Krynitsky, A. I., Metals and Alloys, 4, 79 (1933).

12. Kunin, Zavodyskaya Laboratoriya, 15, 870-2, June, 1949.

13. Lange and Heine, American Foundrymen's Soc., Preprint 52-13.

14. Lips, Foundry Trade Journal, 60, 519-20, June 15, 1939.

15. Liquid Metals Handbook, Edition 2 (1952).

16. Oberhoffer and Wimmer, Stahl und Eisen, 45, 969 (1952).

17. Pillin and Kihlgren, Transactions of AFA, 40, 289 (1932).

18. Porter and Rosenthal, American Foundrymen's Soc., Preprint 52-2.

19. Porter and Rosenthal, American Foundrymen's Soc., Preprint 52-49.

20. Portevin, A. and Bastein, P., Compts Rendue, 194, 559 (1932).

21. Portevin, A. and Bastein, P., Compts Rendue, 194, 850 (1932).

22. Portevin, A. and Bastein, P., Compts Rendue, 202, 1092 (1936).

23. Portevin, A. and Bastein, P., Proceedings of the Institute of British Foundrymen, 29, 88 (1935/6).

24. Portevin, A. and Bastein, P., Journal of Institute of Metals, 54, 45 (1934).

25. Rabinovitch, Doklady Akademic, Nauk, SSSR 54, 395 (1946).

26. Ruff, W., Iron and Steel Institute Carnegie Scholarship Memoirs, 25, 1-39 (1936).

27. Saeger, C. M. and Krynitsky, A. I., Transactions of AFA, 39, 513 (1931).

28. Taylor, Rominski and Briggs, Transactions of AFA, 49, 1-93 (1941).

29. Tedds, D. F. B., Foundry Trade Journal, 88, 443, April 27, 1950.

30. Theilman and Wimmer, Stahl und Eisen, 47, 389-99 (1927).

31. Worthington, J. E., Iron and Steel, 22, 615, Dec., 1949; 23, 9, Jan., 1950.

32. Worthington, J. E., Foundry Trade Journal, 87, 87, July 27, 1950.

33. Taylor and Rightmire, Unpublished Report - to be published in Journal of Institute of Metals.

34. Briggs, C., Metals Handbook, ASM (1948).

35. Lips, Giesserei, 25, 239 (1938).

36. Polyak, E. V. and Sergeev, S. V., Compt. Rend. (Doklady) Acad. Sci. U.R.S.S., 33, 244 (1941).

37. West, T. D., Metallurgy of Cast Iron, Cleveland Printing Co., Cleveland, Ohio (1902).

38. Curry, C., Fonderie Moderne, 18, 71 (1924).

39. Moldenke, Principles of Iron Foundry, McGraw-Hill, New York (1947).

40. Saito and Hayaschi, Proc. College of Eng., Kyoto Imp. Univ., II, 83 (1919); IV, 165 (1924).

41. Kron, E. C. and Lorig, C. H., Trans. of AFA, 47, 583 (1939).

42. Fisher, H. J., Sc. D. Thesis, Yale University (1953).

43. Adams, C. M., Sc. D. Thesis, M.I.T. (1953).

44. Schneider, P., Giesseri No. 6-8, Brutcher Translation No. 3049, 379-81 (1952).

45. Sherwood, T. K. and Reed, C. E., Applied Mathematics in Chemical Engineering, 113-116, McGraw-Hill, New York (1939).

46. Phillips, H. B., Analytical Geometry and Calculus, John Wiley and Sons, New York (1946).

APPENDIX A

NUMERICAL SOLUTION BY MODIFIED EULER TECHNIQUE

Increments were taken in the independent variable Θ. Using Eq. (A-8), values of N were calculated for various friction factors where $N \equiv f(a^4-r_o^4)/8r_o^4(a-r_o)$

Then $$\left(\frac{dL_e}{d\Theta}\right)^2 (1 + NL_e) = V_o^2$$

Values of L_{e_n} for the time Θ_n (which equals n Θ) is given by:

$$L_{e_n} = L_{e_{(n-1)}} + \left(\frac{dL_e}{d\Theta}\right)_{(n-1)} \left[\Theta_n - \Theta_{(n-1)}\right]$$

A modification can be made by recalculating $(dL_e/d\Theta)$ based on the average value of L_e during the interval Θ to $\Theta + \Delta\Theta$.

Successive approximations can be made by using the values of $dL_e/d\Theta$ determined in the previous approximation as follows. Let $L_e^{(k)}$ represent the kth approximation to L_e.

$$L_{e_n}^{(k)} = L_{e_{(n-1)}}^{(k)} + \left(\frac{dL_e}{d\Theta}\right)_{avg}^{(k-1)} \left[\Theta_n - \Theta_{(n-1)}\right]$$

where $$\left(\frac{dL_e}{d\Theta}\right)_{avg}^{(k-1)} = \left[\frac{1}{2}\left(\frac{dL_e}{d\Theta}\right)_n^{(k-1)} + \left(\frac{dL_e}{d\Theta}\right)_{(m-1)}^{(k-1)}\right]$$

The solution converges rapidly as follows:

k	L_f
1	32.76
1 (modified)	28.57
2	29.57
3	29.62
4	29.60

APPENDIX B

SIMPSON'S RULE SOLUTION

This system of solution divides the interval of evaluation (c to d) into 2n parts. With n = d-c/2n and y = g(x)

$$\int_c^d g(x) = \frac{h}{3}\left[y_o + 4y_1 + 2y_2 + 4y_3 \ldots\ldots + 4y_{2n-1} + y_{2n}\right]$$

Using 2n = 4

$$\int_c^d g(x) = \frac{d-c}{12}\left[y_o + 4y_{\frac{3c+d}{4}} + 2y_{\frac{c+d}{2}} + 4y_{\frac{c+3d}{4}} + y_d\right]$$

The assumption is made that $V_e = \left(1 + \frac{\theta}{\theta_f}\right) V_o$

Considering h-type heat transfer Eq. (A-8), Eq. (B-10) becomes:

$$\frac{dL_e}{dr_o} = -\frac{2V_o r_o}{a\beta}\left[1 + \frac{f}{16}\left(\frac{a^4 - r_o^4}{a - r_o}\right)\left(\frac{V_o}{a^2 r_o^4}\right)\right]^{-1/2}$$

Applying Simpson's Rule:

$$L_f = 1/6\,\frac{V_o}{\beta}\left[g(a) + 4g\left(\frac{3a}{4}\right) + 2g\left(\frac{a}{2}\right) + 4g\left(\frac{a}{4}\right) + g(0)\right]$$

where $$g(r_o) = \left[1 + \frac{f}{16}\left(\frac{a^4 - r_o^4}{a - r_o}\right)\frac{V_o}{a^2 r_o^4}\right] r_o$$

$$L_f = 1/6\,\frac{V_o a}{\beta}\; 1 + \left(1 + 21.3\,\frac{V_o f}{\beta}\right)^{-1/2} + \left(1 + 1.76\,\frac{V_o f}{\beta}\right)^{-1/2} + \left(1 + .370\,\frac{V_o f}{\beta}\right)^{-1/2}$$

APPENDIX C

JUSTIFICATION OF ASSUMPTIONS

I. That $r = r_o + \frac{a - r_o}{L_e} L$ (B-6)

The assumption was made that the liquid-solid interface was a conical surface as indicated by the equation above. From the numerical solutions and Eq. (A-8), values of r as a function of L were calculated at various stages in the freezing. The values used for the example were as follows:

$$V_o = 37 \text{ cm/sec}$$

$$\beta = 1.02$$

$$a = 0.197$$

$$f = 0.02$$

In Fig. (B-1), these values are plotted along with the lines indicating the assumed values. For the values above

$$\theta_f = .192 \text{ sec}$$

$$L_f = 34.21 \text{ cm}$$

This approximation (B-6) is used to calculate the friction term of Eq. (B-5). The main contribution to friction (that is, the major throttling) occurs in the portion of the tube having the smallest radius. Fig. (B-1) shows that assumption (B-6) is especially valid in the small radius portion of the tube. In Fig. (B-1) note that actual values do not deviate from the assumed values appreciably until more than 87% of the flow is complete.

II. That friction factor remains approximately constant during flow.

The case being treated concerns a pure metal at the m.p. The flow is turbulent under most conditions, hence,

$$f = 0.185 \, N_{Re}^{-0.20}$$

$$\frac{\Delta f}{f} = 0.20 \left| \frac{\Delta N_{Re}}{N_{Re}} \right| \qquad \text{(II-1)}$$

where N_{Re} = Reynolds Number = $\frac{2V_r\rho}{\mu}$

Now $$V = V_e \frac{a^2}{r^2}$$

and $$V_e = \frac{V_o}{\theta_f} (\theta_f - \theta) \qquad \text{(C-13)}$$

For h-type heat transfer $$r^2 = a^2 - a\beta\theta \qquad \text{(A-8)}$$

Combining, $$N_{Re} = \frac{2a^2 V_o \rho}{\mu \theta_f} \frac{\theta_f - \theta}{(a^2 - a\theta)^{1/2}} \qquad \text{(II-2)}$$

As θ changes:

$\frac{\theta}{\theta_f}$	$\frac{\Delta N_{Re}}{N_{Re}}$	$\frac{\Delta f}{f}$
0	0	0
0.25	.135	.027
0.50	.293	.059
0.75	.500	.100

The table above indicates that f changes very slowly as θ/θ_f increases. Even at $\theta/\theta_f = 0.75$, (at which time more than 86 per cent of flow is complete) the friction factor has changed only 10 per cent. Under most operating conditions this change in f will not appreciably affect the results.

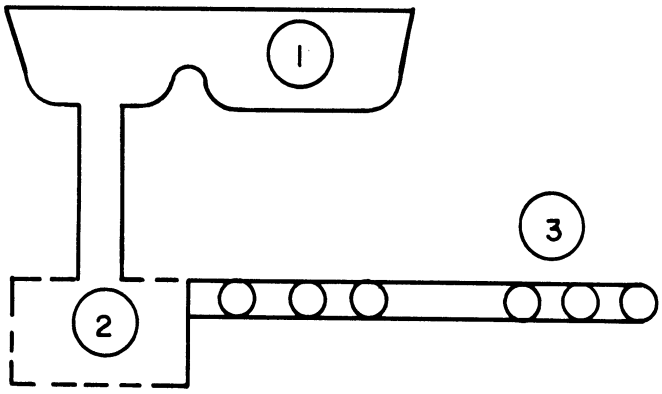

CASTING SYSTEM FOR FLUIDITY SPIRAL

FIGURE 1

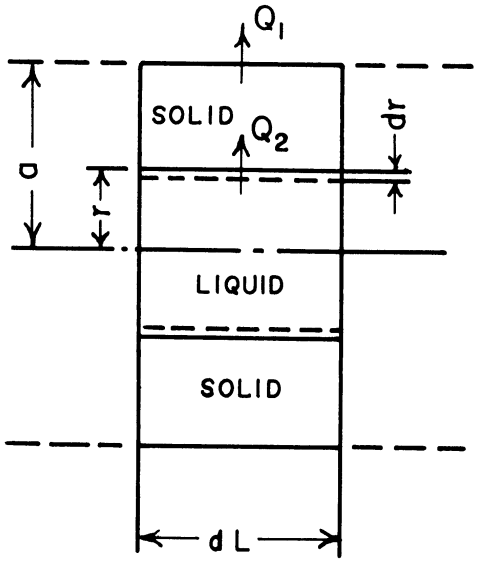

DIFFERNTIAL ELEMENT OF TUBE

FIGURE 2

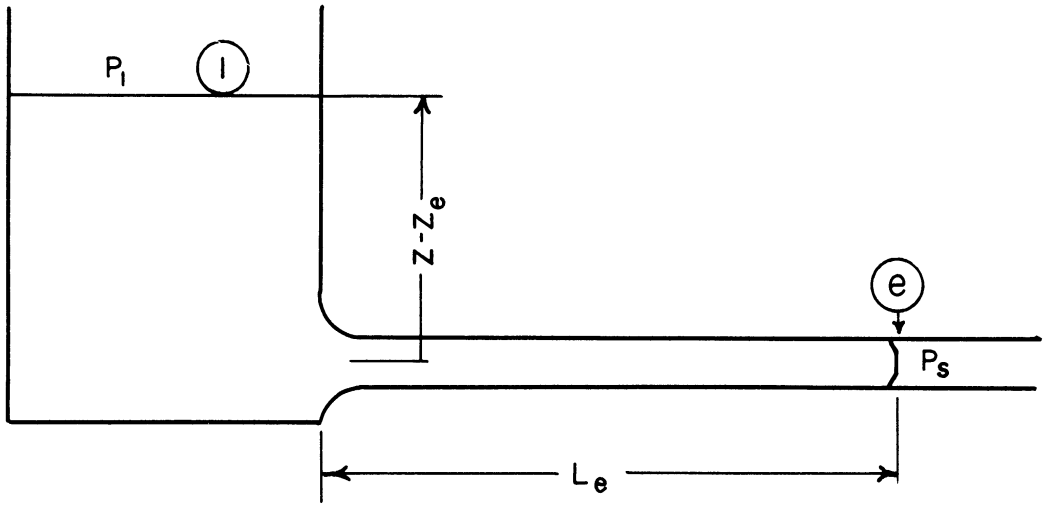

FLUID SYSTEM

FIGURE 3

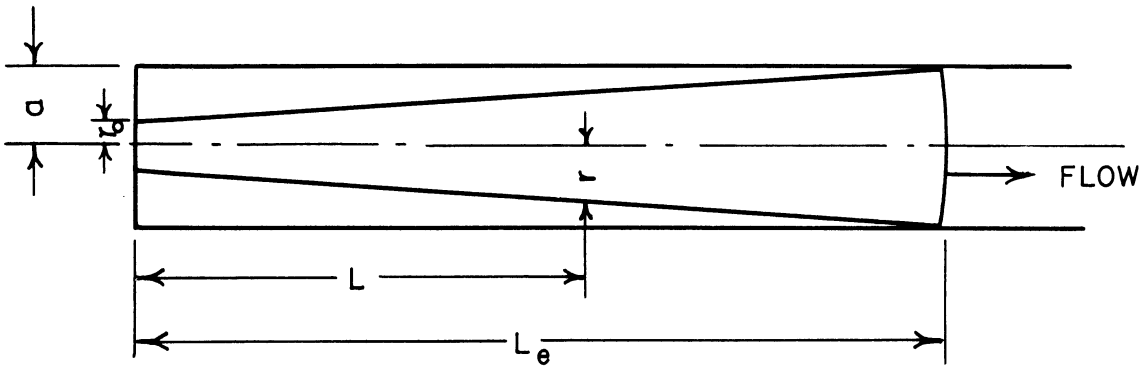

CROSS-SECTION OF TUBE WITH SOLIDIFICATION

FIGURE 4

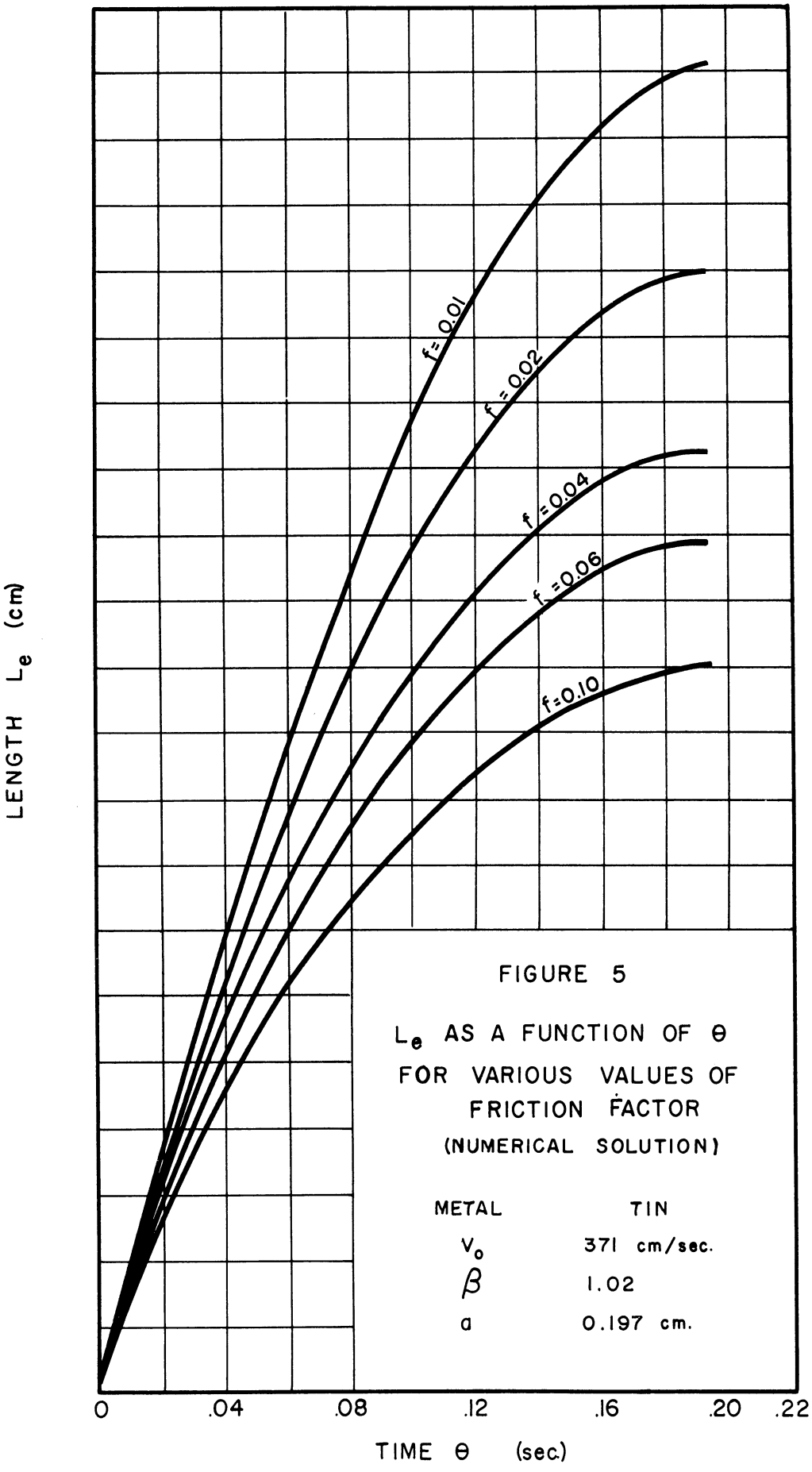

FIGURE 5

L_e AS A FUNCTION OF θ FOR VARIOUS VALUES OF FRICTION FACTOR (NUMERICAL SOLUTION)

METAL	TIN
V_o	371 cm/sec.
β	1.02
a	0.197 cm.

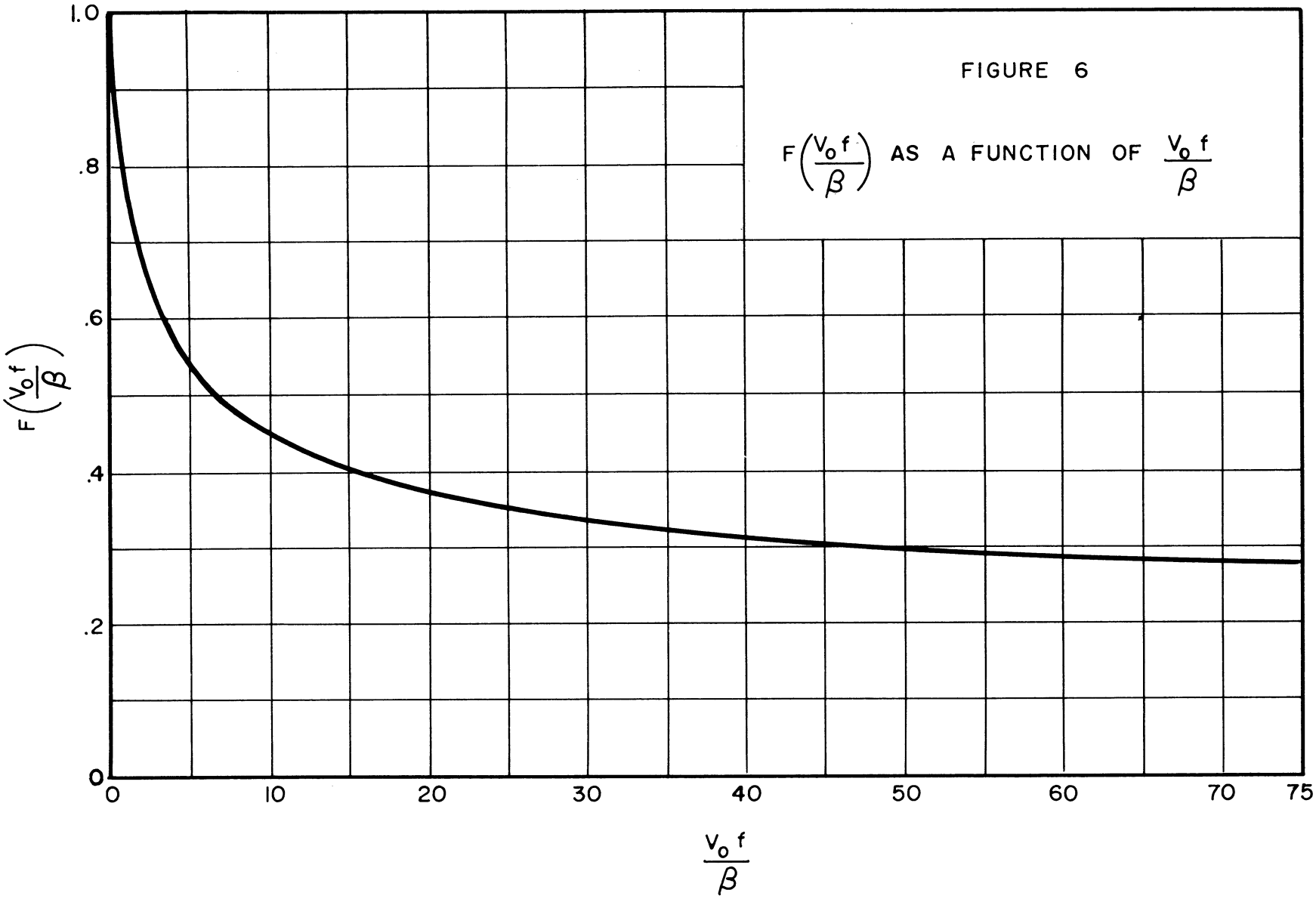

FIGURE 6

$F\left(\frac{V_0 f}{\beta}\right)$ AS A FUNCTION OF $\frac{V_0 f}{\beta}$

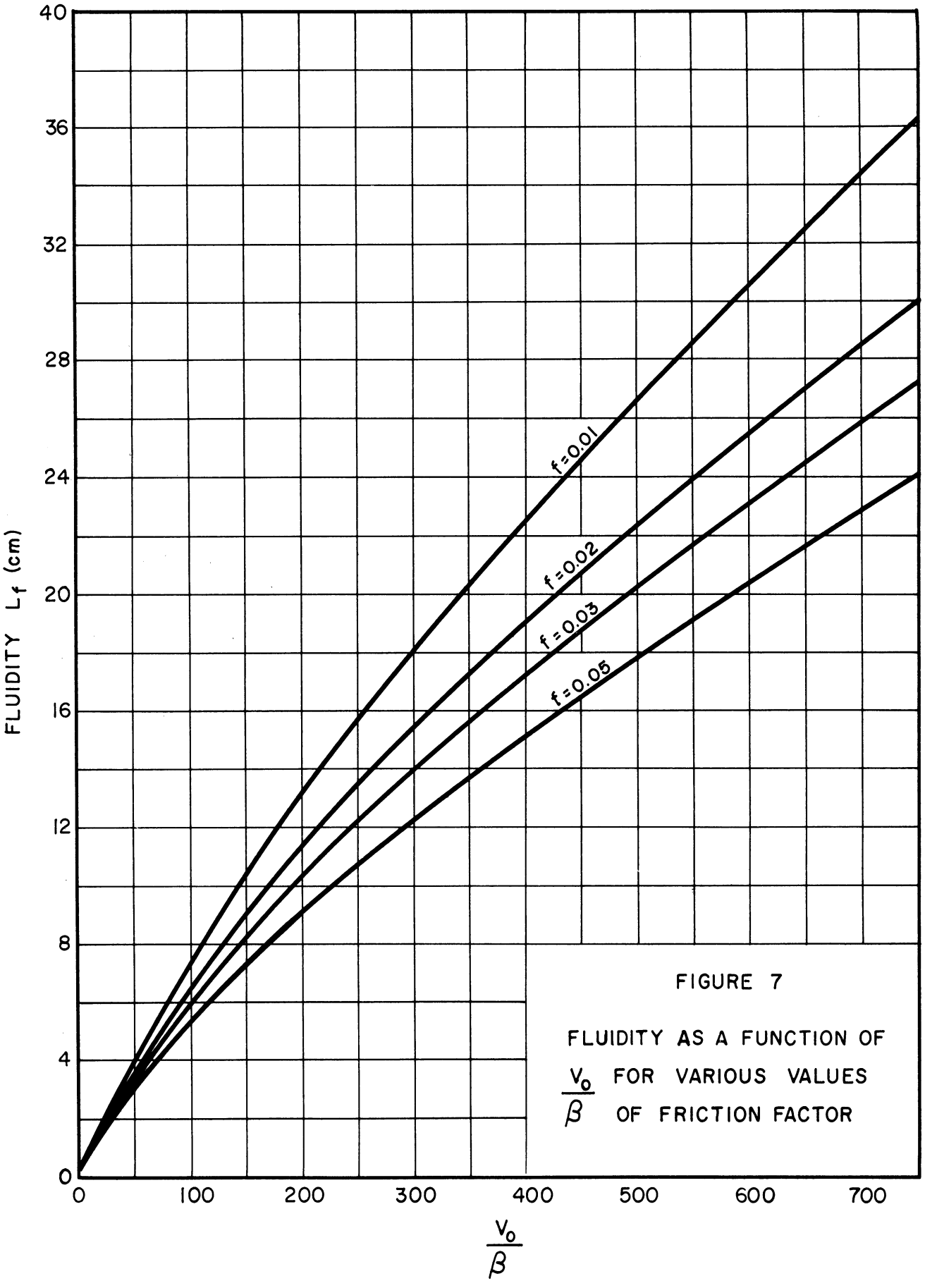

FIGURE 7

FLUIDITY AS A FUNCTION OF $\frac{V_0}{\beta}$ FOR VARIOUS VALUES OF FRICTION FACTOR

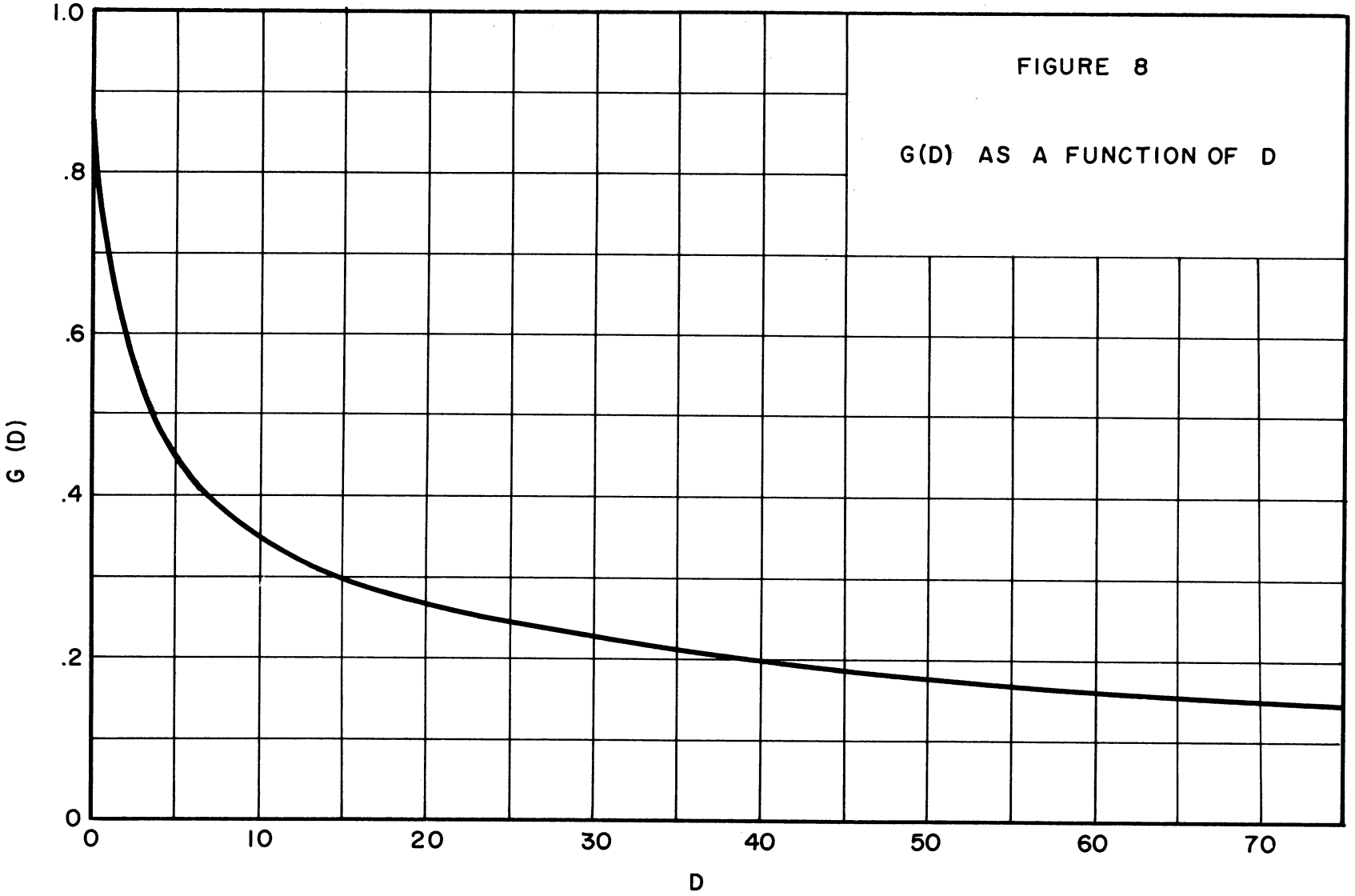
FIGURE 8
G(D) AS A FUNCTION OF D
1.0
.8
.6
.4
.2
0
G (D)
0
10
20
30
40
50
60
70
D

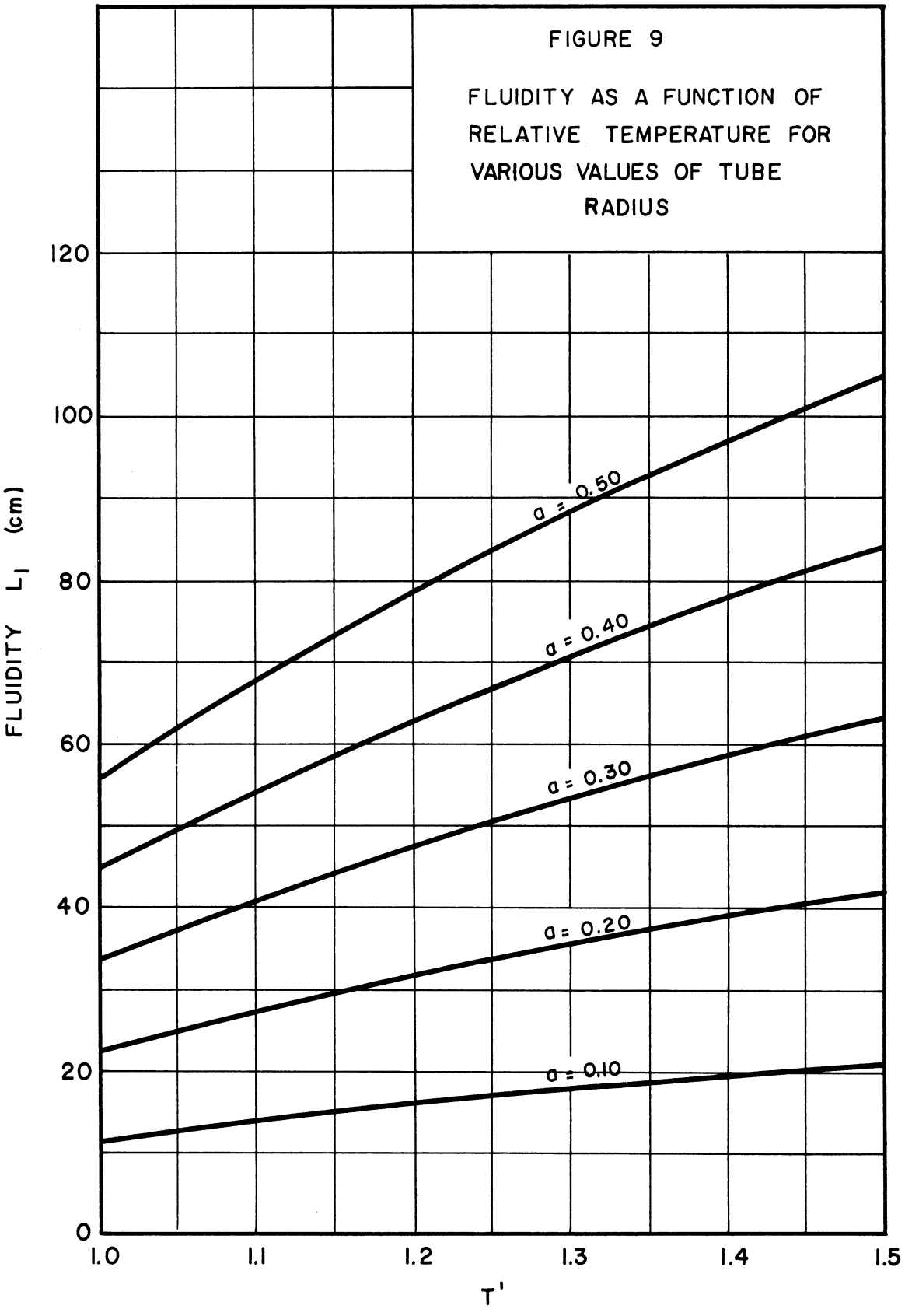
FIGURE 9
FLUIDITY AS A FUNCTION OF RELATIVE TEMPERATURE FOR VARIOUS VALUES OF TUBE RADIUS
FLUIDITY L_1 (cm)
120
100
80
60
40
20
0
a = 0.50
a = 0.40
a = 0.30
a = 0.20
a = 0.10
1.0
1.1
1.2
1.3
1.4
1.5
T'

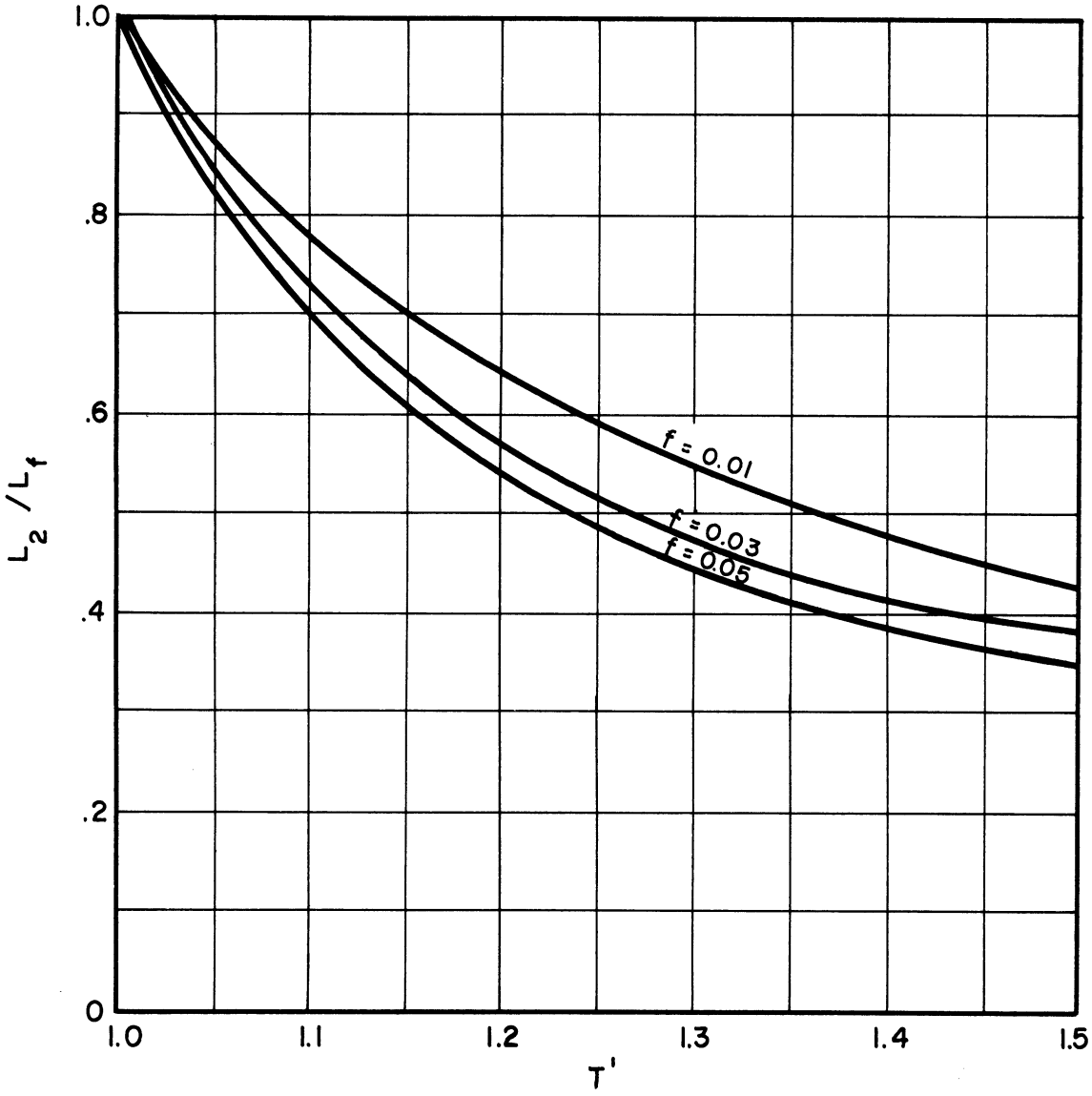

L_2/L_f AS A FUNCTION
OF RELATIVE TEMPERATURE

FIGURE 10

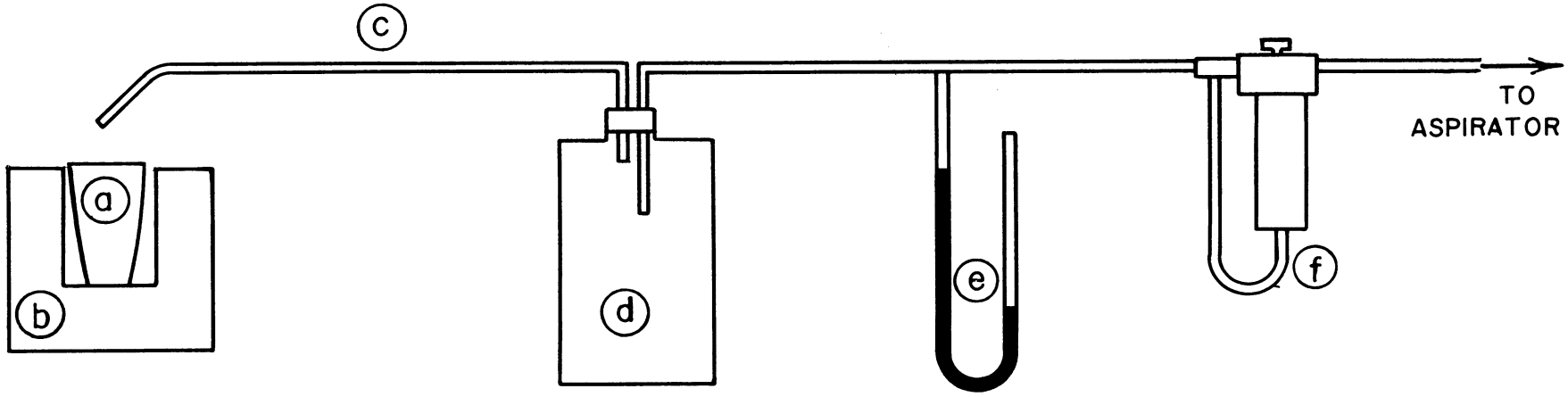

a) Crucible of Metal
b) Electric Resistance Furnace
c) Fluidity Test Channel
d) Pressure Resevoir
e) Manometer
f) Cartesian Manostat

SCHEMATIC DIAGRAM OF EQUIPMENT

FIGURE II

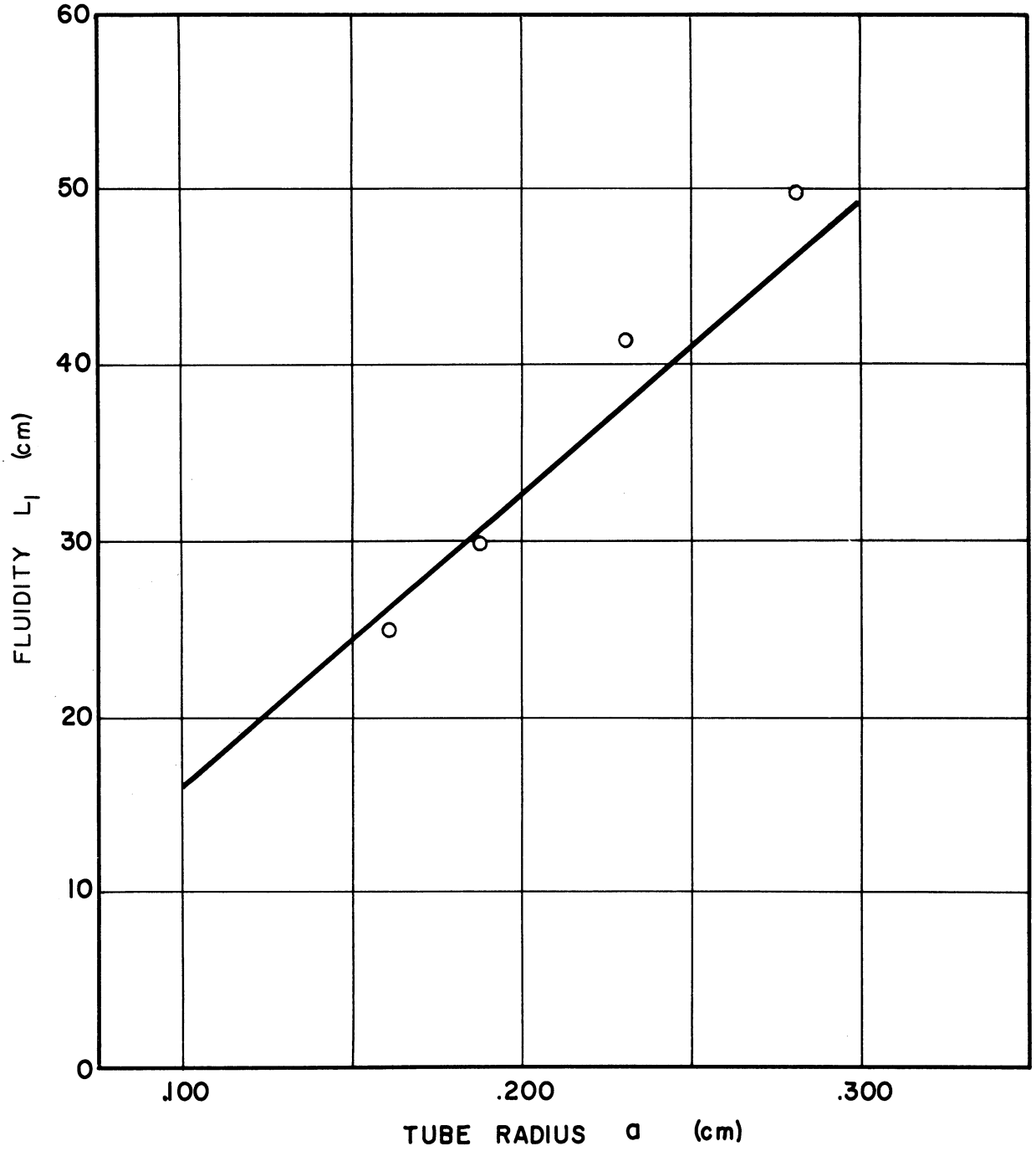

FLUIDITY OF TIN AT MELTING POINT AS A FUNCTION OF TUBE RADIUS

FIGURE 12

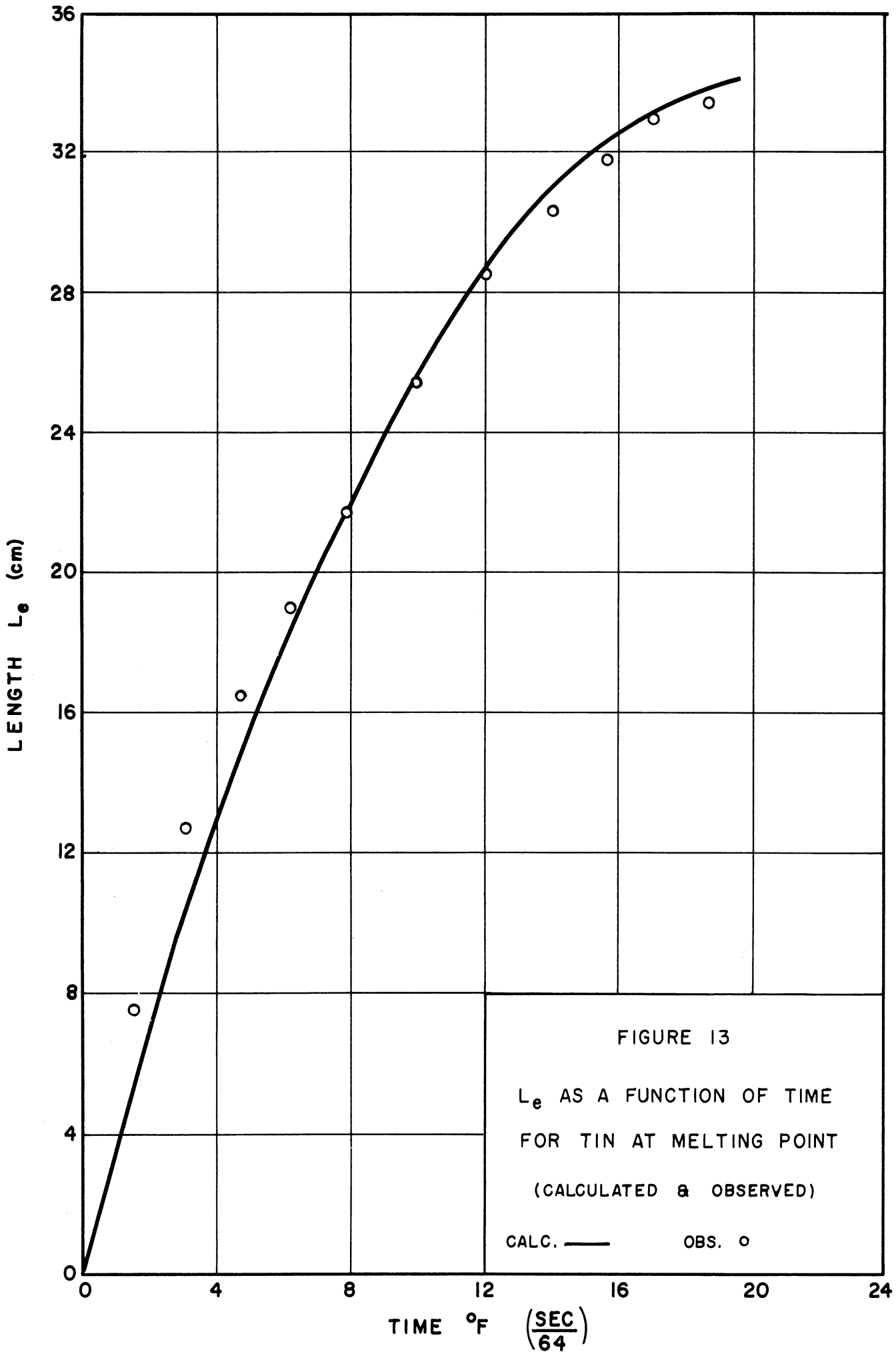
36
32
28
24
20
16
12
8
4
0
LENGTH L_e (cm)
0
4
8
12
16
20
24
TIME °F $\left(\frac{SEC}{64}\right)$
FIGURE 13
L_e AS A FUNCTION OF TIME
FOR TIN AT MELTING POINT
(CALCULATED & OBSERVED)
CALC. ——
OBS. o

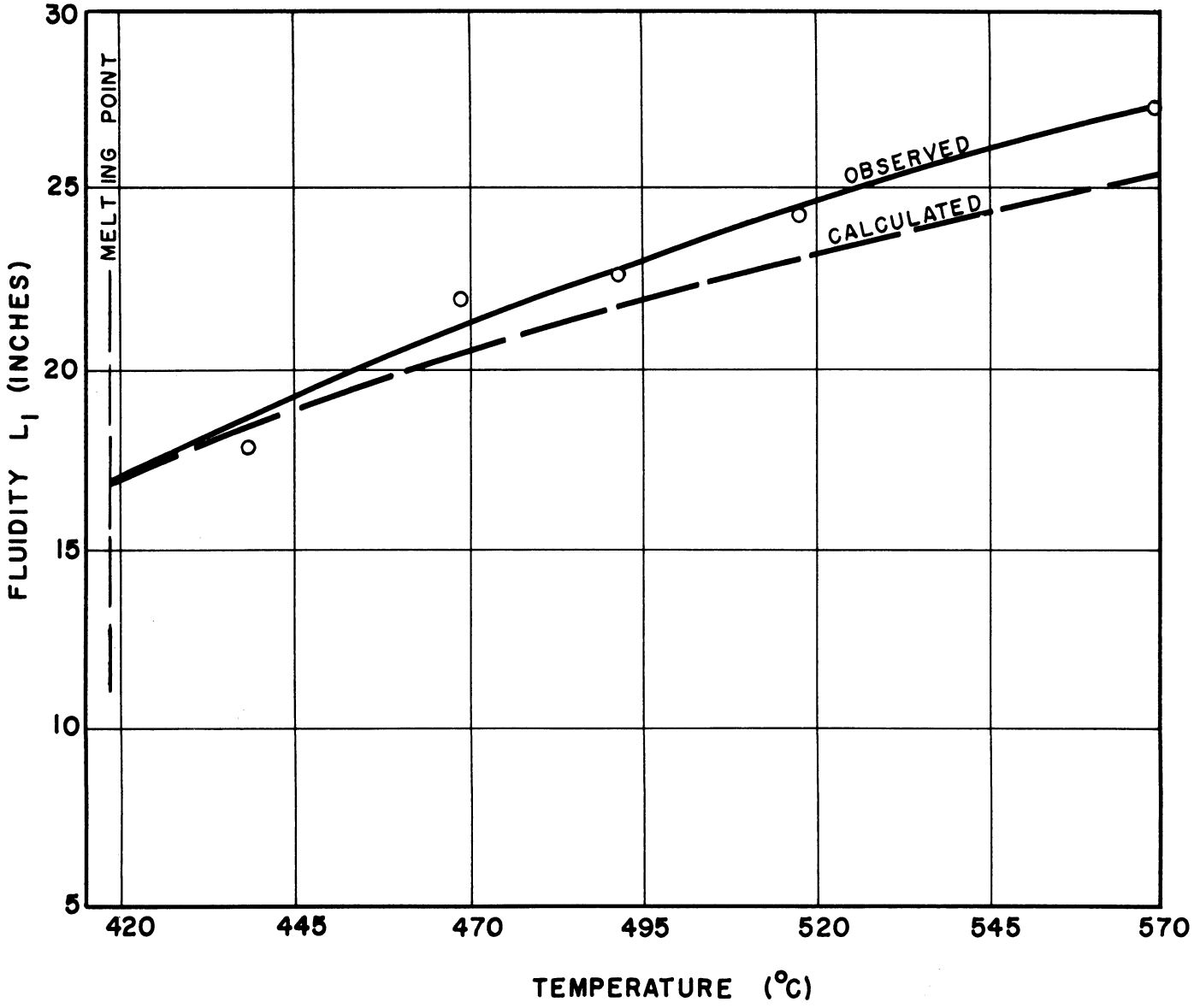

FLUIDITY OF ZINC AS A FUNCTION OF TEMPERATURE IN ALUMINUM TUBES (I. D. = .152")

FIGURE 14

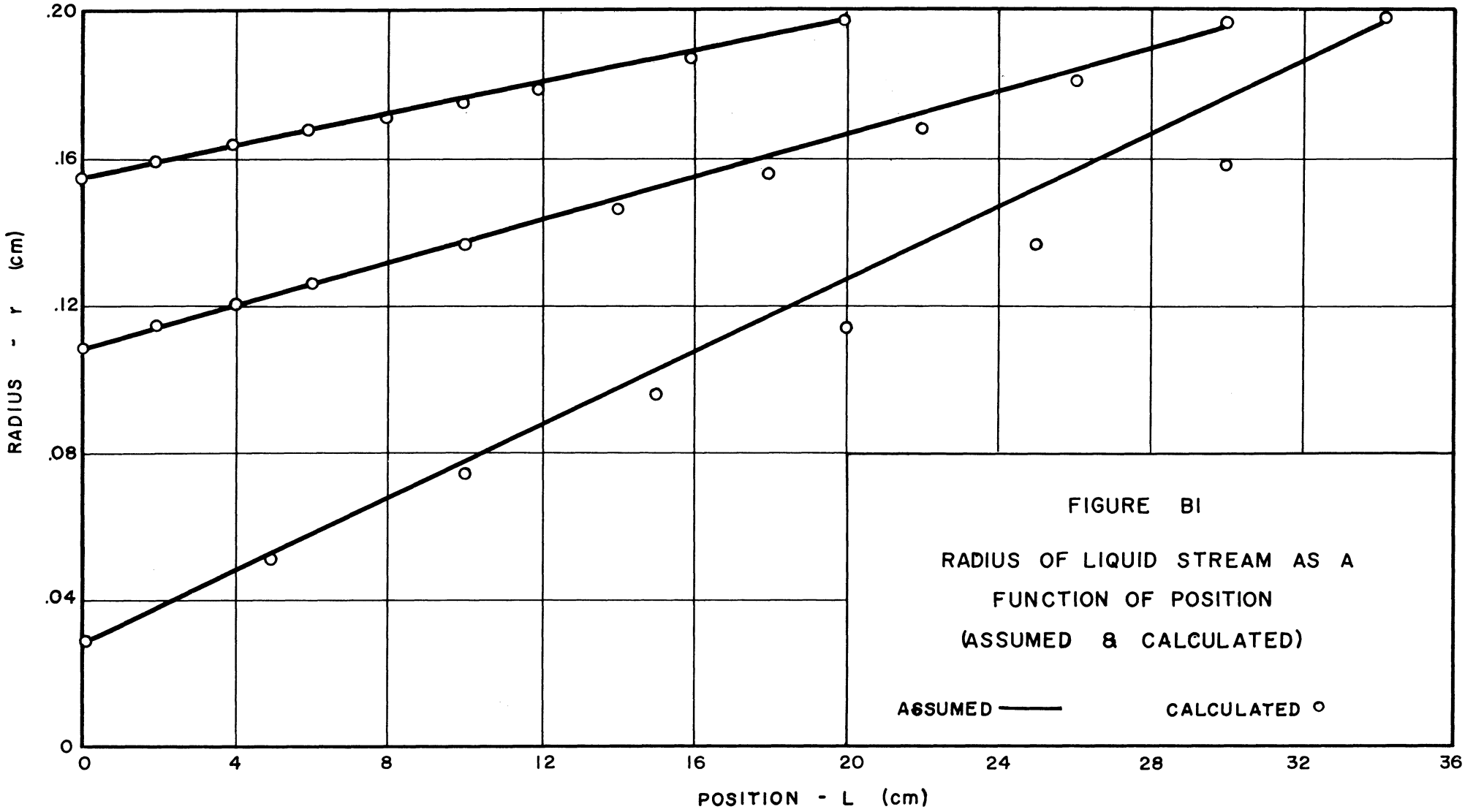
.20
.16
.12
.08
.04
0
RADIUS - r (cm)
0
4
8
12
16
20
24
28
32
36
POSITION - L (cm)
FIGURE BI
RADIUS OF LIQUID STREAM AS A FUNCTION OF POSITION (ASSUMED & CALCULATED)
ASSUMED
CALCULATED

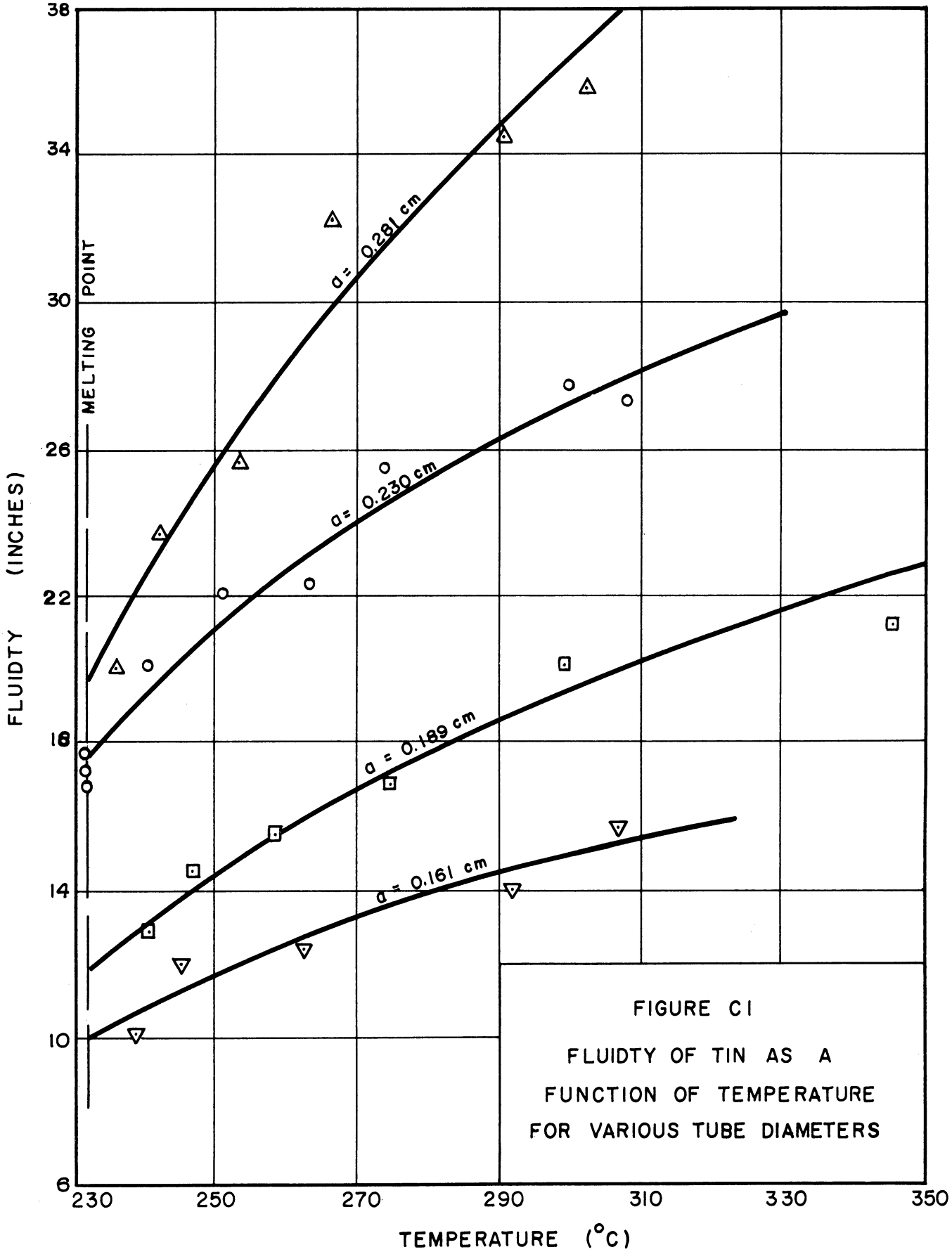

FIGURE C1

FLUIDTY OF TIN AS A FUNCTION OF TEMPERATURE FOR VARIOUS TUBE DIAMETERS

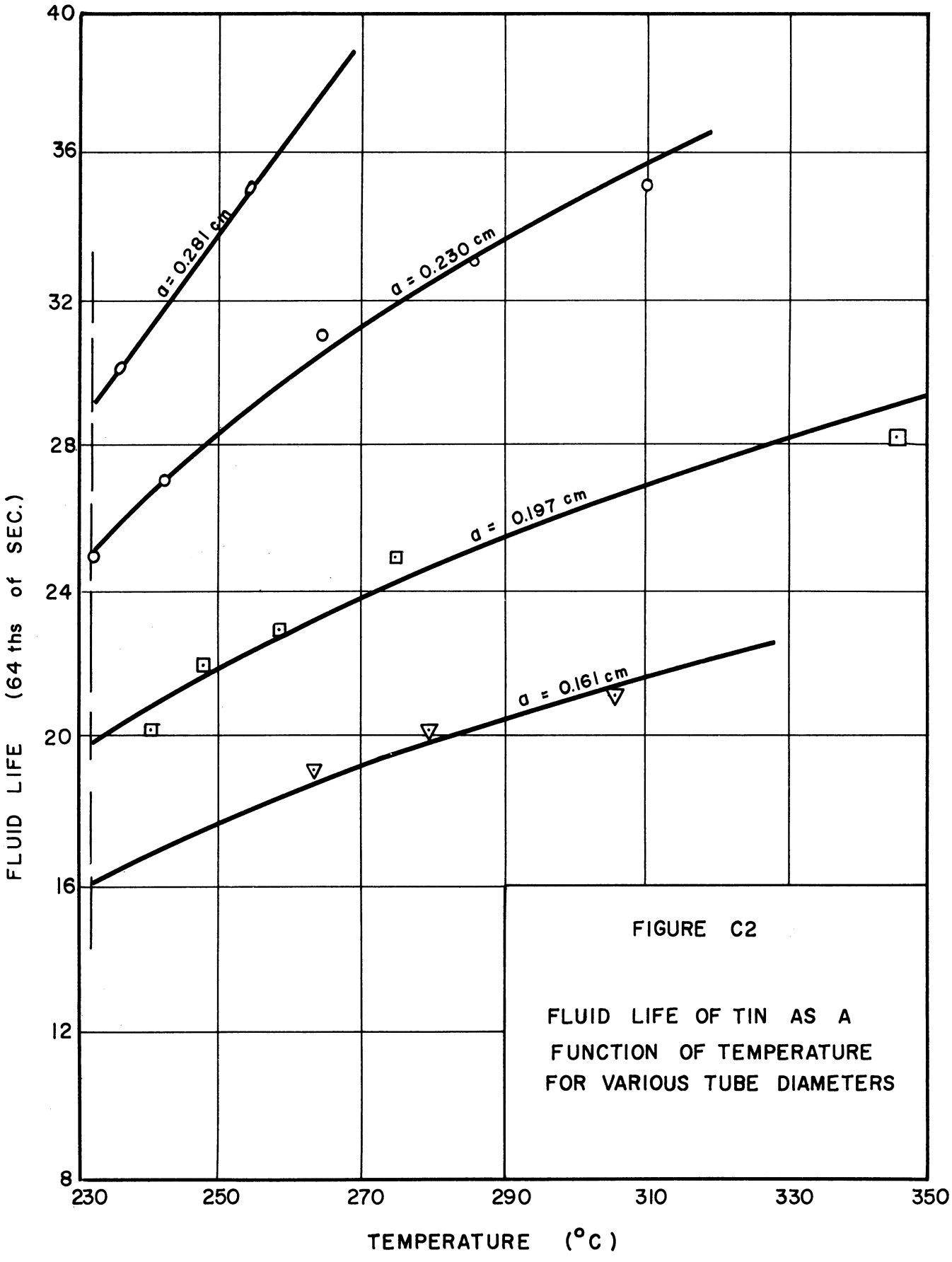

FIGURE C2

FLUID LIFE OF TIN AS A FUNCTION OF TEMPERATURE FOR VARIOUS TUBE DIAMETERS